

Electronic Supplementary Information (ESI)

An insight into the preferential substitution and structural repair in Eu²⁺-doped whitlockite-type phosphors-combining experiment and theoretical calculation

Zhongxian Qiu,^a Wenli Zhou,^{*a} Zhongyun Ma,^{*b} Jilin Zhang^a, Shixun Lian^a, and Ru-
Shi Liu^{*cd}

^a. Key Laboratory of Chemical Biology and Traditional Chinese Medicine Research, Ministry of Education, College of Chemistry and Chemical Engineering, Hunan Normal University, Changsha 410081, China. E-mail: chemwlzhou@hunnu.edu.cn

^b. Department of Chemistry, Key Laboratory of Environmentally Friendly Chemistry and Applications of Ministry of Education, Xiangtan University, Xiangtan 411105, China. E-mail: zhyma@xtu.edu.cn

^c. Department of Chemistry, National Taiwan University, Taipei 106, Taiwan. E-mail: rsliu@ntu.edu.tw

^d. Department of Mechanical Engineering and Graduate Institute of Manufacturing Technology, National Taipei University of Technology, Taipei 106, Taiwan

S1. Phase Composition and Rietveld Refinement.

The composition and phase purity of the as-synthesized TCPK_x-Eu phosphors were identified by powder XRD determinations. The diffraction patterns of the samples with different K contents are shown in **Fig. S1a**. All the samples keep the iso-structure with the initial whitlockite TCP. With increasing *x* values from 0 to 1.0, as exhibited in the magnified patterns, in the range of 27.2-34.7 ° (**Fig. S1b**), regular shift of the diffraction peaks can be detected, which implies the formation of a series of continuous solid solution. The peaks ascribed to (2 1 4) and (2 2 0), respectively, lattice planes shift gradually to the lower diffraction angles. Meanwhile, the change of the location of the peak at about 31 ° is not that obvious and even a tendency to higher angle is recognized. The results indicate a heterogeneous variation of the cell parameters. A further illustration is displayed in **Table S1**. With the growth of K content, a linear increase of parameter *a* (= *b*) but a linear decrease of parameter *c* are obtained through Rietveld refinements. The good fitting coefficients further validate the phase purity of the as-prepared samples. The atomic parameters of the endpoint compounds TCP and TCPK are demonstrated in **Table S2** and **Table S2**, respectively.

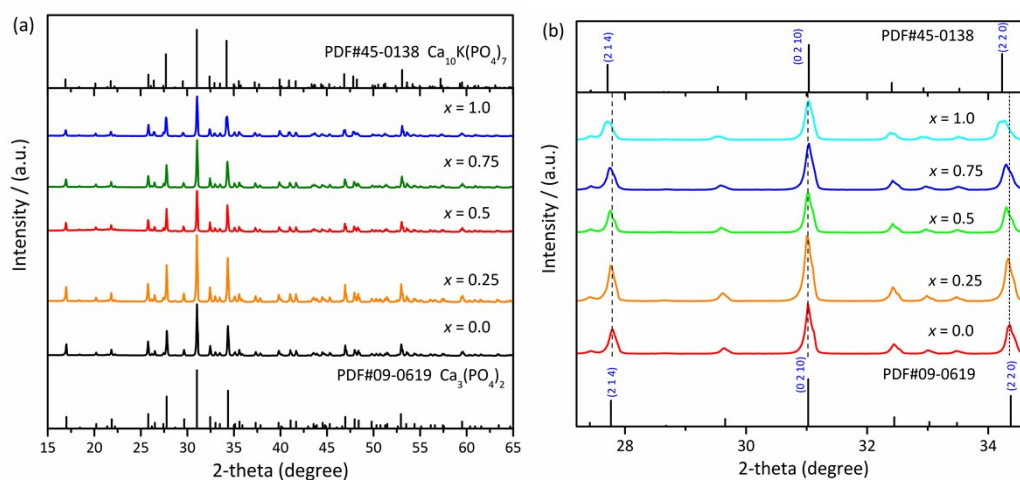


Figure S1. (a) Representative XRD patterns of TCPK_x-Eu (*x* = 0.0 – 1.0) phosphors and (b) the

magnified patterns in the range from 27.2 to 34.7 °.

Table S1. Crystallographic Parameters from powder Rietveld Refinement for $\text{Ca}_{10.5-0.5x}\text{K}_x(\text{PO}_4)_7\text{:Eu}$ samples.

	$x = 0$	$x = 0.25$	$x = 0.50$	$x = 0.75$	$x = 1.00$
Space Group	<i>R3c</i>	<i>R3c</i>	<i>R3c</i>	<i>R3c</i>	<i>R3c</i>
$a/\text{Å}$	10.4375(9)	10.4415(3)	10.4479(2)	10.4531 (4)	10.4579(6)
$b/\text{Å}$	10.4375(9)	10.4415(3)	10.4479(2)	10.4531 (4)	10.4579(6)
$c/\text{Å}$	37.3881(8)	37.3767(4)	37.3558 (7)	37.3406(4)	37.3268 (4)
α°	90	90	90	90	90
β°	90	90	90	90	90
γ°	120	120	120	120	120
cell volume/ Å^3	3527.49(2)	3529.18(2)	3532.29(9)	3533.02(4)	3535.41(7)
χ^2	1.336	1.896	1.323	1.743	1.592
R_{wp}	7.71%	7.53%	6.90%	8.65%	8.18%
R_{p}	5.96%	5.73%	5.43%	6.62%	6.31%

Table S2. Atomic parameters of refined β -Ca₃(PO₄)₂ cell.

Atom	Ox.	Wyck.	Site	S.O.F.	x/a	y/b	z/c	U [Å ²]
Ca1	2	18b	1	1	0.72420	0.85570	0.16640	0.0060
Ca2	2	18b	1	1	0.61820	0.82130	-0.03260	0.0040
Ca3	2	18b	1	1	0.72930	0.85210	0.06110	0.0133
Ca4	2	6a	3.	0.43	0	0	-0.08680	0.0172
Ca5	2	6a	3.	1	0	0	0.73440	0.0095
P1	5	6a	3.	1	0	0	0.00060	0.0158
P2	5	18b	1	1	0.68540	0.85910	0.86840	0.0092
P3	5	18b	1	1	0.65130	0.84520	0.76720	0.0058
O1	-2	18b	1	1	0.73740	-0.08650	-0.09030	0.0407
O2	-2	18b	1	1	0.77430	0.78540	0.85800	0.0325
O3	-2	18b	1	1	0.72760	0.00800	0.84740	0.0165
O4	-2	18b	1	1	0.52420	0.76330	0.86080	0.0127
O5	-2	18b	1	1	0.60300	-0.04320	0.77980	0.0000
O6	-2	18b	1	1	0.57230	0.68970	0.78360	0.0037
O7	-2	18b	1	1	0.07060	0.89570	0.77490	0.0071
O8	-2	18b	1	1	0.63210	0.82620	0.72630	0.0186
O9	-2	18b	1	1	0.00930	0.86390	-0.01320	0.0434
O10	-2	6a	3.	1	0	0	0.0402(3)	0.0092

Table S3. Atomic parameters of refined Ca₁₀K(PO₄)₇ cell.

Atom	Ox.	Wyck.	Site	S.O.F.	x/a	y/b	z/c	U [Å ²]
Ca1	2	18b	1	1	0.39840	0.18660	0.02770	0.0146
Ca2	2	18b	1	1	0.39260	0.18830	0.13320	0.0074
Ca3	2	18b	1	1	0.18060	0.38390	0.10170	0.0095
Ca5	2	6a	3.	1	1/3	2/3	0.03500	0.0084
K	1	6a	3.	1	0	0	0.04810	0.0514
P1	5	6a	3.	1	0	0	0.13570	0.0149
P2	5	18b	1	1	0.13450	0.31290	0.00230	0.0081
P3	5	18b	1	1	0.48710	0.47560	0.06750	0.0079
O1	-2	6a	3.	1	0	0	0.17340	0.0213
O2	-2	18b	1	1	0.01470	0.15160	0.12120	0.0163
O3	-2	18b	1	1	0.08550	0.27170	0.04510	0.0210
O4	-2	18b	1	1	0.23110	0.24560	-0.00880	0.0130
O5	-2	18b	1	1	-0.00940	0.28080	-0.02020	0.0096
O6	-2	18b	1	1	0.23700	0.48360	-0.00680	0.0144
O7	-2	18b	1	1	0.41130	0.56500	0.07410	0.0024
O8	-2	18b	1	1	0.50900	0.47570	0.02610	0.0104
O9	-2	18b	1	1	0.64190	0.54210	0.08170	0.0187
O10	-2	18b	1	1	0.37760	0.31310	0.07950	0.0166

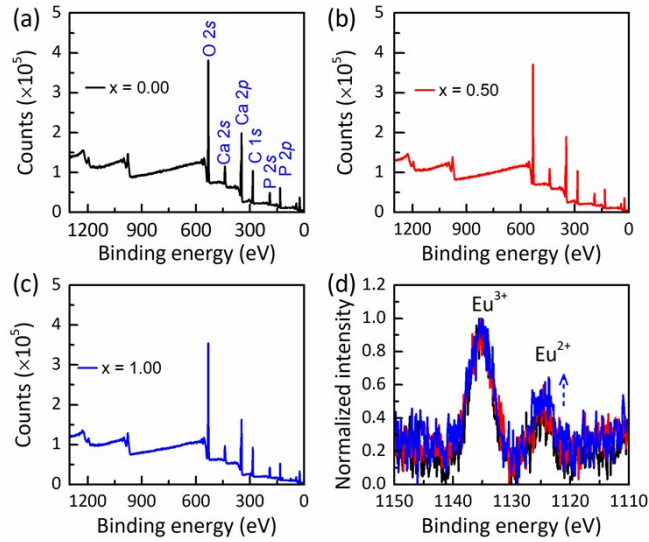
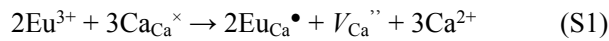


Figure S2. XPS measurements of TCPK_x-Eu samples with different K content (a-c), Eu3d core levels deconvoluted to discriminate the two valent states (d), and K2p core levels (e): the black, green and red curves correspond to the samples with $x = 0, 0.5$ and 1.0 , respectively.

Considering the charge balance mechanism, two Eu^{3+} ions can substitute for three Ca^{2+} ions, resulting in a vacancy defect with two negative charges V_{Ca}'' and two positive defects $\text{Eu}_{\text{Ca}}^\bullet$. Then, the vacancy defect acts as the donor of electrons and the two $\text{Eu}_{\text{Ca}}^\bullet$ become the acceptors. The electrons may be transferred from V_{Ca}'' to $\text{Eu}_{\text{Ca}}^\bullet$ sites by phonon-assisted processes, resulting in the reduction of Eu^{3+} to Eu^{2+} ions. The whole process (S1-S3) is presented as follows:



In $\text{Ca}_3(\text{PO}_4)_2:\text{Eu}$ system, there is a lot of vacancy defect on the M4 sites, resulting in difficult reduction of Eu^{3+} to Eu^{2+} ions according to the reaction (S4), because the V_{Ca}^\times may competitively capture the freedom electrons which can be used to reduce the Eu^{3+} ions.

After K^+ doping, the K^+ will occupy the vacancy site, causing the amount of vacancy defect extreme decreasing (5). As a result, under reduction condition, the Eu^{3+} could be easily reduced to Eu^{2+} ions. The changes of the Eu^{2+}/Eu^{3+} ratio at a fixed europium doping concentration are show in the XANES (**Fig. 2c**) and XPS spectra (**Fig. 3b**).

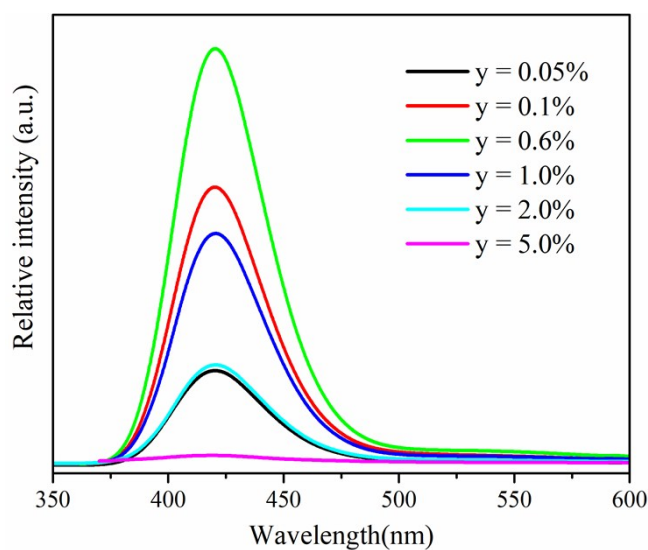


Figure S3. Photoluminescent spectra of TCP: yEu^{2+} under excitation of 330 nm.

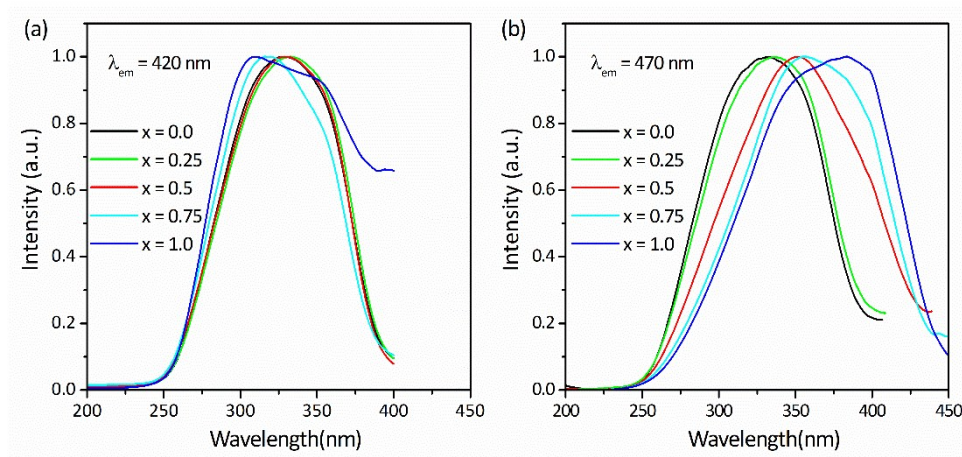


Figure S4. Normalized excitation spectra of TCPK_x-Eu phosphors monitored at 420 nm (a) and 470 nm (b).

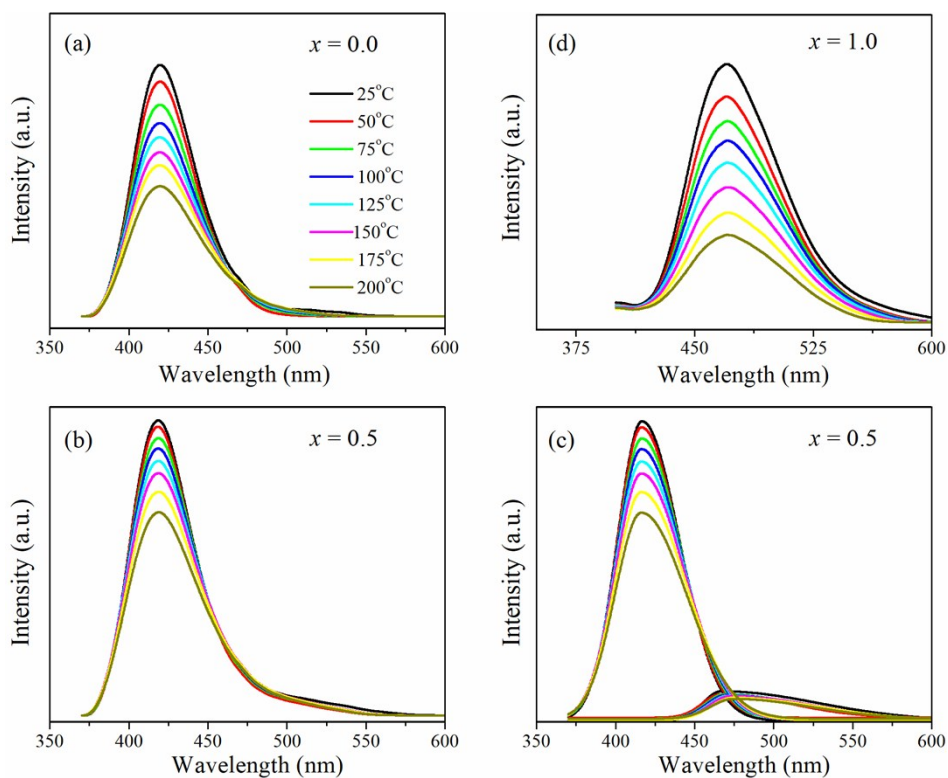


Figure S5. PL spectra of TCPK_x-Eu phosphors at various temperatures: (a) $x = 0$, (b) $x = 0.5$, (c) fitted emission spectra of $x = 0.5$ samples and (d) $x = 1.0$.

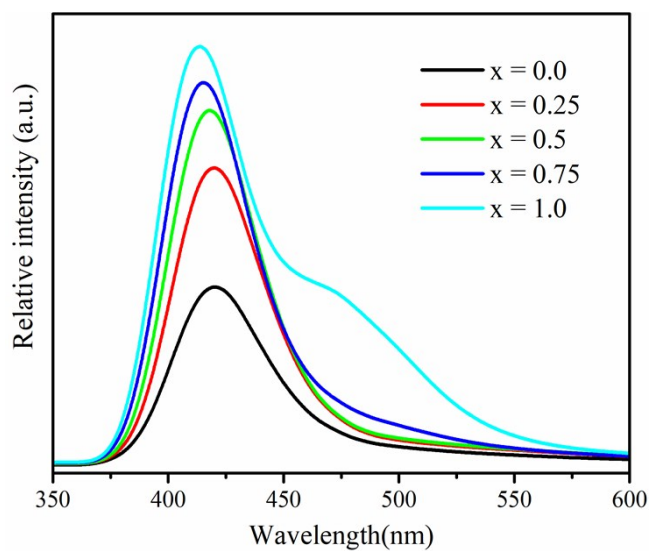


Figure S6. Photoluminescent spectra of TCPK_x:0.05%Eu²⁺ under excitation of 330 nm.

Table S4. The comparison of calculated cell parameters of TCP and TCPK by DFT.

	$a/\text{\AA}$	$b/\text{\AA}$	$c/\text{\AA}$	Volume/ \AA^3
TCP	10.547	10.547	37.708	3632.78
TCPK	10.608	10.608	37.561	3660.34
Changes	+0.575%	+0.575%	-0.391%	+0.759%

Table S5. The comparison of average M-O bond length in TCP and TCPK.

	Ca(1)-O ₇ / \AA	Ca(2)-O ₈ / \AA	Ca(3)-O ₈ / \AA	M(4)-O ₉ / \AA	Ca(5)-O ₆ / \AA
TCP	2.4566	2.5070	2.5474	2.8431	2.2779
TCPK	2.4527	2.5229	2.5565	3.0333	2.3035

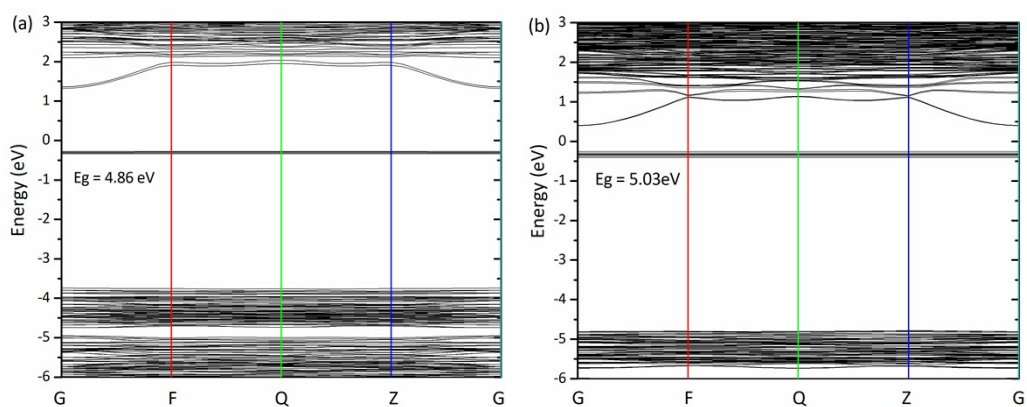


Figure S7. Band structures of TCP-Eu (a) and TCPK-Eu (b) with Eu²⁺ at Ca(4) and Ca(3) site, respectively.

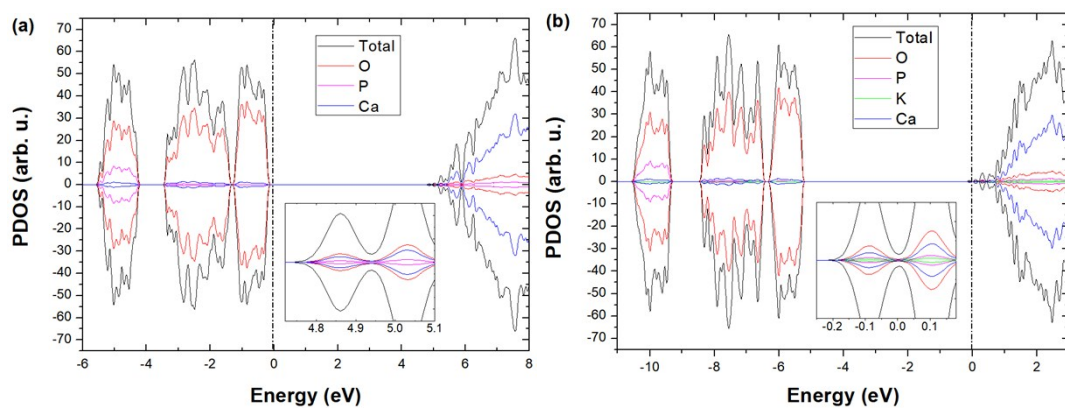


Figure S8. PDOS of TCP (a) and TCPK (b).

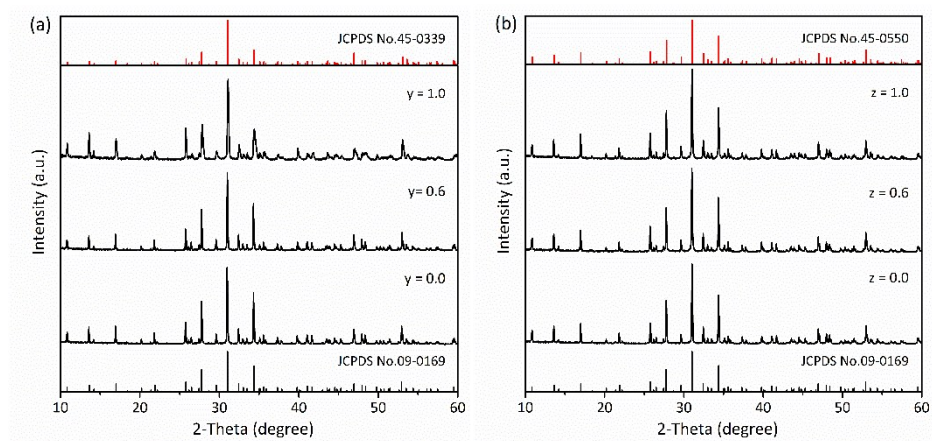


Figure S9. Representative XRD patterns of TCPNa_y-Eu (a) and TCPLi_z-Eu (b) phosphors